

Selecting Best Mother Wavelets for Suppressing Non-Homogeneous Noise Patterns in Magnetic Resonance (MR) Images

Rashid Hussain, Abdul Rehman Memon, Adnan Ahmed Siddiqui, Syed Wasif Ali Shah

Faculty of Engineering Science and Technology, Hamdard University, Karachi 74600, (PAKISTAN)

ABSTRACT

Mother wavelet has been studying for various imaging applications including de-noising, compression and segmentation. Performance Analysis of mother wavelet requires immediate attention for non-homogeneous noise perspective. In this study, wavelet thresholding based technique is used to de-noise the Magnetic Resonance (MR) images. Sure Shrink method is used for selecting the thresholds. Brain MR images of a subject with Multiple Sclerious disease have been selected for the investigation. The subject brain MR Images contains three abnormal white spots. This study is an attempt to analyze various mother wavelets with different synthesized noise patterns in the brain MR Images. Results showed that the bi-orthogonal function *bior3.7* performed better for most of the noise suppression cases. Based on the study, it is proposed that the selection of right Mother Wavelet for de-noising, improves the quality of post-process image, consequently making it possible to improve the accuracy of diagnostic imaging.

KEY WORDS: De-noising, Compact Support, Orthogonality, Symmetry, Multiple Sclerious.

1. INTRODUCTION

Mother wavelet is one of the fundamental concepts used in wavelet analysis. Unlike Fourier analysis, wavelet analysis decomposes a signal not in terms of cosine and sine but in wavelet function called mother wavelet. The main idea of the mother wavelet is to provide a source function to create more wavelets by changing the translation and dilation properties of mother wavelets. Mathematically it is represented as “ ψ ”. The continuous wavelet transform $X_{CWT}(T, s)$ of the given signal $x(t)$ can be given as equation (1),

$$X_{CWT}(\tau, s) = \frac{1}{\sqrt{|s|}} \int x(t) \bullet \psi^* \left(\frac{t - \tau}{s} \right) dt \quad (1)$$

Where the wavelet translation is represent as “ τ ” and the dilation is represent as “ s ”. The translation “ τ ” provides the location window of mother wavelet in time domain. The scaling “ s ” provides the coverage of the wavelet spectrum in time domain. It is inversely related with the bandwidth in frequency domain. In order to reduce number of wavelets to represents signal/image, finite number of scaling functions used to cover the entire spectrum.

The wavelet series expansions of function $f(x)$ relative to wavelet $\psi_{j,k}(x)$ and scaling function $\phi_{j,k}(x)$ can be given as equation (2) [1,2,3],

$$f(x, y) = \sum_k c_{j_0}(k) \phi_{j_0,k}(x) + \sum_{j=j_0}^{\infty} \sum_k d_j(k) \Psi_{j,k}(x) \quad (2)$$

The first part of the wavelet series expansions of function $f(x)$ corresponds to **approximation** of the function at j_0 level by the linear combination of scaling function $\phi_{j,k}(x)$, and second part of the wavelet series expansions of function $f(x)$ corresponds to **details** of the different levels contained in the function by the linear combination of wavelet function $\psi_{j,k}(x)$ at gradually higher scales $j_0+1, j_0+2, j_0+3, \dots$

Scaling or approximation coefficients can be given as equation (3),

$$c_{j_0}(k) = \langle f(x), \phi_{j_0,k}(x) \rangle = \int f(x) \phi_{j_0,k}(x) dx \quad (3)$$

*Corresponding Author: Rashid Hussain, Faculty of Engineering Science and Technology, Hamdard University Karachi, 74600, (PAKISTAN). Email: hussain_rashid@hotmail.com Phone: +92(314)220-9995

Wavelet or detail coefficients can be given as equation (4),

$$d_j(k) = \langle f(x), \psi_{j_o,k}(x) \rangle = \int f(x)\psi_{j_o,k}(x)dx \tag{4}$$

Using mother wavelet, the signal undergoes through a series of translations (shifts) and dilations (scaling) to capture features at local level. Further details can be seen at [4, 5].

This process results in wavelet coefficients representing the correlation between the wavelet and local sections of the signal both in frequency and time domain. This property of the wavelet analysis makes it ideal for analyzing the signal with abrupt changes.

1. PROPERTIES OF MOTHER WAVELETS

In the following section properties of mother wavelets will be presented.

Compact support of the mother wavelet measures the effective width of the function; it leads to the efficient implementation. A narrow width of the function helps for fast computation, on the other hand a wider width of the function suitable for finer frequency resolution, which makes it efficient for image de-noising. Another important property of mother wavelet is the orthogonality. Orthogonal functions have zero correlation (no overlap with each other), while bi-orthogonal functions have non zero correlation (some overlap with each other) when computing the transform. Unlike fourier analysis, wavelet transforms can be symmetrical or asymmetrical. The choices of symmetric and asymmetric influence the performance of mother wavelets in term of image de-noising and segmentation. Vanishing moments of the wavelet represents the mathematical relationship for the coefficients to be satisfied. This property represents the smoothness present in both frequency and time domain of wavelet functions [4, 5].

2. MOTHER WAVELETS AND ITS DE-NOISING CAPABILITIES

Today a large numbers of mother wavelets are available for signal and image processing. Some of the prominent include Haar, Daubechies, Symlet, Morlet, Coiflet and Discrete Meyer. The following section will briefly discuss some of the mother wavelets used in the study.

3.1 Haar: haar

Haar function is one of the oldest and the fundamental mother wavelet. It is representing by the sequence of rescaled “square-shape” functions. It is operates on the signal by calculating the sum and differences of adjacent elements. Due to its discontinuing nature, haar wavelet generally shows worst performance for compression and de-noising applications [6].

3.2 Daubechies: dbN

Daubechies function was proposed by Ingrid Daubechies. It can be orthogonal or bi-orthogonal depending on the scaling and wavelet function coefficients. Compared to Haar function, Daubechies are relatively complex and requires more computations. Due to its better frequency response, it shows better de-noising results[7].

3.3 Symlet: symN

Symlet function belongs to near symmetrical orthogonal and bi-orthogonal family proposed by Ingrid Daubechies as modifications to the db function [7].

3.4 Coiflet: coifN

The Coiflet function is more symmetrical then Daubechies, developed by Ingrid Daubechies as a request of Coifman [7]. Compare to Daubechies function, Coiflet are relatively symmetrical.

3.5 Bi-orthogonal: biorN

The Bi-orthogonal is symmetrical and almost orthogonal function. This mother wavelet provides near orthogonal and symmetrical function. It generally performs better for de-noising applications [8].

Mother wavelets and its de-noising capabilities are summarized in Table1.

Table 1: De-noising analysis of various Mother Wavelets

Mother Wavelets	Symmetry	Orthogonality	Compact Support	Description
Haar	Symmetrical	Yes	Orthogonally supported	Simple and Fast. Because of the discontinuities it cannot be used for de-noising applications.
Daubechies	Asymmetrical	Yes	Orthogonally supported	Because of overlapping filter it can be used for de-noising.
Symlet	Near Symmetrical	Yes	Orthogonally supported	It has highest numbers of vanishing moments.
Coiflet	Near Symmetrical	No	Bi-orthogonally supported	It has highest numbers of vanishing moments.
Bi-orthogonal	Symmetrical	No	Bi-orthogonally supported	Bi-orthogonal has advantage over orthogonal wavelet due to its Linear Phase property

4. IMAGE QUALITY ASSESSMENT METHODS

In the following section image quality assessment methods will be presented. Three image index metrics are used to analyze the performance of mother wavelets:

4.1 Mean Square Error (MSE)

MSE is the figure of merit, computed by taking the square of cumulative errors, as shown in equation (5),

$$MSE = \sum_{i=1}^x \sum_{j=1}^y \frac{(A_{ij} - B_{ij})^2}{x * y} \quad (5)$$

Where A_{ij} and B_{ij} represent the pixel values of original and reconstructed images respectively. It can be expressed as the mean of square distance between pixel of the original image A_{ij} and pixel of the reconstructed image B_{ij} .

4.2 Mean Absolute Error (MAE)

MAE is another figure of merit, computed by taking the average of cumulative errors, as shown in equation (6),

$$MAE = \sum_{i=1}^x \sum_{j=1}^y \frac{|A_{ij} - B_{ij}|}{x * y} \quad (6)$$

4.3 Peak Signal to Noise Ratio (PSNR)

PSNR is the measure of peak error in the pixel values of two sets of images, as shown in equation (7),

$$PSNR = 10 \log^* \left(\frac{255^2}{MSE} \right) \quad (7)$$

There is an inverse relation between MSE and PSNR: the higher values of MSE and MAE translate as a lower value of PSNR. In de-noising analysis, it means that there exists a higher value of error between the original and reconstructed image. A lower value of MSE, means that the performance is relatively better.

Two types of noise distributions are prominent in MR image: Gaussian and Rician [9]: the former is generally data independent and relatively easy to remove while the later is data dependent and requires better de-noising techniques.

5. IMAGE PATTERNS IN MULTIPLE SCLERIOUS DISEASE

Diagnosing Multiple Sclerious disease requires utmost care; especially the early detection is far more challenging. Identifying malignant patterns from benign patterns could possibly hamper the early detection. This problem could become severe if the MR Image corrupted with small bursts of noise. Various conventional de-noising techniques have been used to suppress noise with the assumption that the random noise is uniformly distributed over the entire image [10, 11, 12, 13]. In real images, bursts of noise with different intensities are possible. Proper diagnosis of Multiple Sclerious disease is possible with expert opinion aided with better diagnostic tools. This study is an attempt to investigate the de-noising performance of various Mother Wavelets under non-homogeneous and homogeneous noisy conditions.

6. PROCEDURE

The procedure describes performance analysis of mother wavelets in the presence of noise patterns:

1. Magnetic resonance (MR) image of a subject with Multiple Sclerious disease has been selected for this study. The subject brain MRI contains three prominent abnormal white spots as shown in Figure 1.
2. Presence of noise especially in the form of burst may results in false negative. If these noises stay with image patterns, it could hamper the detection of malignant areas. Therefore, it is important to understand the effects of noise pattern in MRI. The focus of the research is to investigate the effects of bursts on the de-noising performance. For this purpose, images synthesized with non-homogeneous noise bursts at various regions including two of the white spots. The images contain Gaussian noise at different levels (0.020 dB to 0.030 dB). Similar Synthesis has been performed in previous studies [14, 15].
3. First level decomposition of brain MRI has been performed to detect near invisible noise bursts using Mallat's Multi-Resolution Analysis (MRA). The MRA analyzes the signal at different frequency bands with different resolutions by

decomposing the signal into a coarse approximation and detail information. The process of obtaining the approximation and detail coefficient is termed as decomposition [1].

4. Wavelet Thresholding based technique is used to de-noise the image. Sure Shrink method is used for selecting thresholds. The basic criterion here is to remove or reduce noisy coefficients. Threshold co-efficient process limits the selection of incorrect threshold coefficients among those chosen for the wavelet reconstruction. The idea behind wavelet thresholding coefficient is to compare with a given threshold λ , if its magnitude is below certain value it will set to zero value (hard thresholding.) otherwise kept for analysis based on threshold rules (soft thresholding) [16].
5. Image quality matrix Mean Square Error (MSE), Mean Absolute Error (MAE) and Peak Signal to Noise Ratio (PSNR) have been used for accessing the performance of original, noisy and de-noised image.

7. RESULTS AND DISCUSSION

The Matlab ® based analysis has been performed on MR image with various noise patterns, as shown in Figure 1. First image contains three noise bursts of various intensities. All images have a uniform dimension that is 256 x 256 pixels. The size of noise burst is approximately 30 x30 pixels. Small size of malignant areas may consist of even few pixels, which poses a challenge for de-noising technique The MR Image is also synthesized with a random noise uniformly distributed across the entire image. During the investigation of adaptive thresholding for image de-noising, it was noticed that discrete mother Wavelet, together with soft thresholding, yielded optimal results.

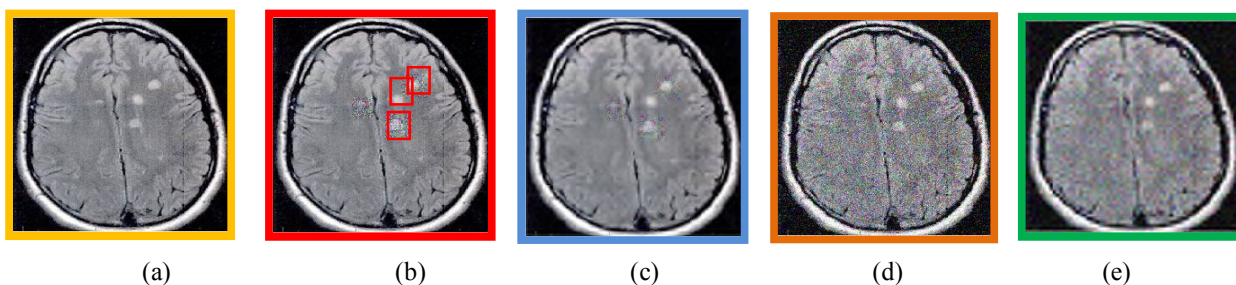


Figure 1: (a) Original MR Image (b) Original image corrupted with different burst of noise (0.020 db, 0.025db and 0.030 db) as shown in red boxes (c) De-noised image (non-homogeneous) (d) Original image corrupted with homogeneous noise (0.020 db) (e) De-noised image (homogeneous).

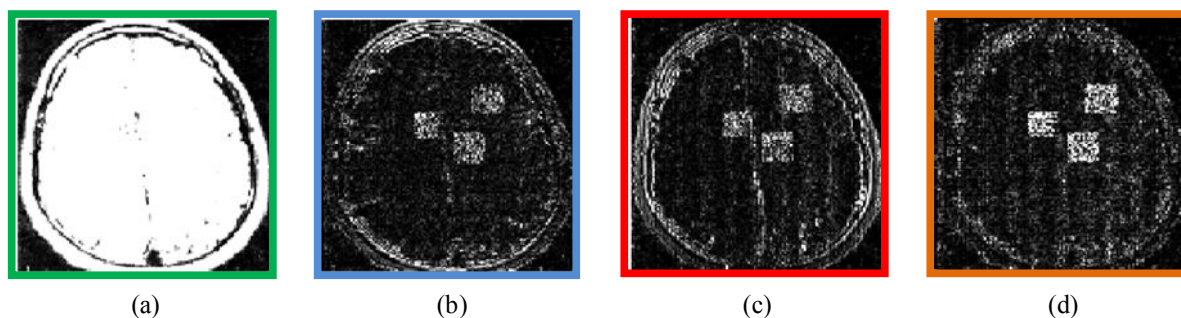


Figure 2: First level decomposition of brain MRI (a) Approximation A1 (b) Horizontal Detail H1 (c) Vertical Detail V1 (d) Diagonal Detail D1.

The *detection* of patterns in an image with noise bursts using multi-resolution analysis [1] are shown in Figure 2. The outcome of this procedure is obtained in the *Diagonal Detail D1* components of multi-level decomposition as shown in shown in Figure 2(d). Similar details can be obtain using *Horizontal Detail H1* and *Vertical Detail V1* components of multi-level decomposition, as shown in shown in Figure 2(b) and Figure 2(c) respectively. This analysis could be used to identify noise patterns, which otherwise, goes undetected by visual assessments. Figure 2(a) shows *Approximation A1* of decomposed image.

The effects of non-homogeneous noise patterns on the de-noising performance of various mother wavelets are shown in Table 2 and Figure 3. Starting first with Daubechies wavelet functions *db1* and *db2*; the image quality index Mean Square Error (MSE1) is the highest, which shows that *db1* underperformed for de-noising. With second attempt, Coiflet wavelet functions *Coif1*, *Coif2* and *Coif3*; the image quality index MSE1 is in average range. With third attempt, bi-orthogonal wavelet functions *bior1.5*, *bior3.7*, *bior4.4*, *bior5.5* and *bior6.8*; the image quality index is in average range, the mother wavelet *bior 3.7* showed better results for suppressing noise patterns. With fourth attempt, symlet wavelet functions *sym3*, *sym4*, *sym5* and

sym6; the MSE1 is in lowest range and comparable to Bi-orthogonal functions, The mother wavelet *sym3* showed better results for suppressing noise patterns.

Table 2: Comparison Analysis for Non-homogeneous Noisy Image

Mother Wavelet/ Image Index	MSE1	MAE1	PSNR1	MSE2	MAE2	PSNR2
<i>db:1</i>	71.8475	3.4381	29.6007	507.7065	10.1237	21.1087
<i>db:2</i>	61.3497	3.2037	30.2867	459.4238	9.679	21.5427
<i>Coif:1</i>	58.5234	3.1425	30.4915	453.4992	9.615	21.599
<i>Coif:2</i>	54.348	3.016	30.813	439.324	9.4589	21.737
<i>Coif:4</i>	54.3628	3.022	30.8118	434.1257	9.4097	21.7886
<i>Bior:1.5</i>	68.0226	3.3105	29.8383	510.252	10.0521	21.087
<i>Bior:3.7</i>	47.5166	2.7896	31.3963	397.5438	9.0481	22.1709
<i>Bior:4.4</i>	56.0548	3.0572	30.6787	438.5198	9.4437	21.7449
<i>Bior:5.5</i>	58.6768	3.1242	30.4801	439.6161	9.4671	21.7341
<i>Bior:6.8</i>	54.5406	3.0273	30.7976	431.9535	9.383	21.8104
<i>Sym:3</i>	47.8155	3.088	30.5928	442.5836	9.4737	21.7048
<i>Sym:4</i>	55.492	3.0489	30.7225	441.9369	9.4711	21.7112
<i>Sym:5</i>	55.7434	3.0453	30.7029	446.6712	9.5054	21.6649
<i>Sym:6</i>	55.097	3.0387	30.7535	436.6075	9.4206	21.7639

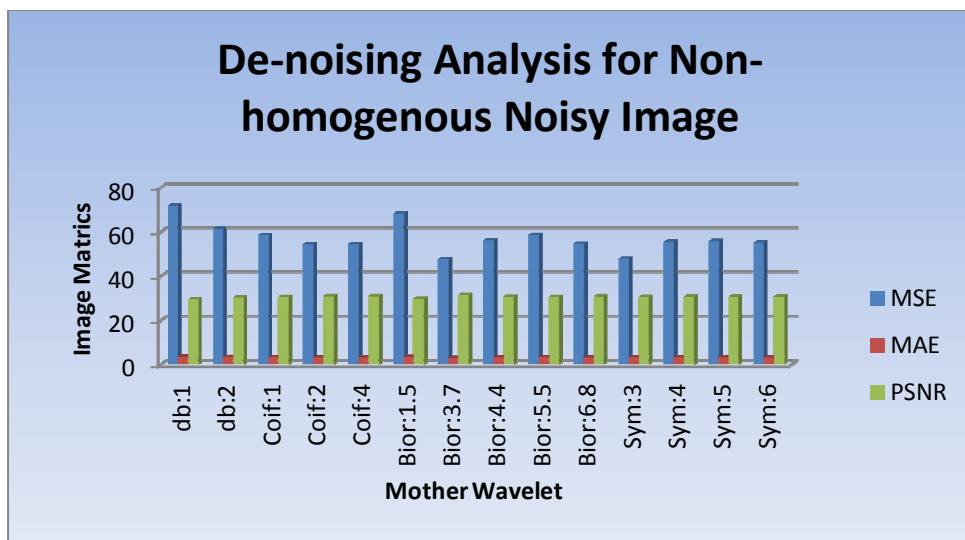


Figure 3: Comparison Analysis for Non-homogeneous Noisy Image

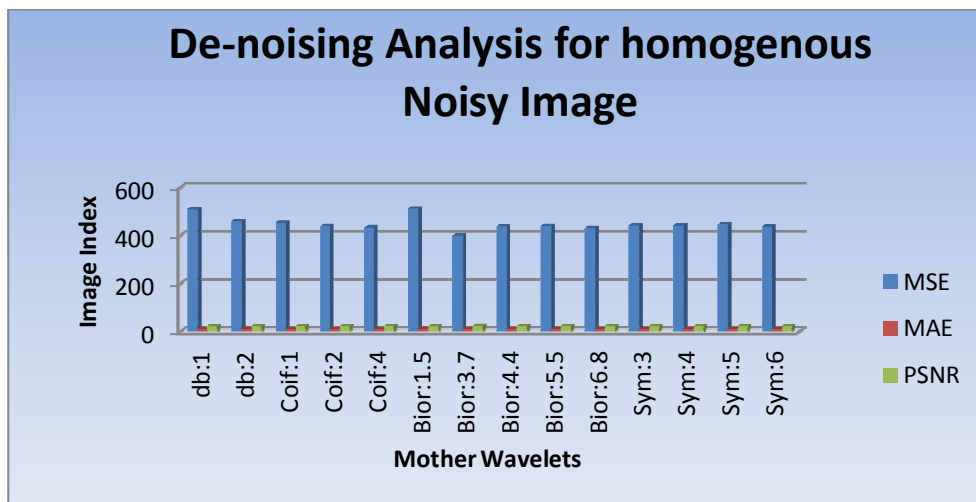


Figure 4: Comparison Analysis for homogeneous Noisy Image

The effects of homogeneous noise on the de-noising performance of various mother wavelets are shown in Table 2 and Figure 4. Starting first with Daubechies wavelet functions *db1* and *db2*; the image quality index Mean Square Error (MSE2) is the highest, which shows that *db1* underperformed for de-noising. With the second attempt, Coiflet wavelet functions *Coif1*, *Coif2* and *Coif4*; the image quality index MSE2 is in average range. With the third attempt, bi-orthogonal wavelet functions *bior1.5*, *bior3.7*, *bior4.4*, *bior5.5* and *bior6.8*; the image quality index is in average range, the Mother Wavelet *Bior 3.7* showed better results for suppressing noise patterns, *Bior1.5* showed worse performance for suppressing noise. With fourth attempt, Symlet Wavelet functions *sym3*, *sym4*, *sym5* and *sym6*; the MSE2 is in lowest range and comparable to bi-orthogonal functions. It is observed that the Mean Absolute Error (MAE) is fairly uniform for both analyses: Homogeneous and non-homogeneous noise suppression.

8. CONCLUSION

Various mother wavelets have been analyzed in the presence of noise patterns. This experimental study showed how adversely noise burst affects the performance of wavelet based de-noising. Results concluded that *BiorN* and *SymletN* functions demonstrated better de-noising capabilities. Bi-orthogonal wavelets have been a good choice because it is relatively smooth and symmetrical. The multi-resolution analysis makes it possible to identify pattern of interests in Multiple Scleriosis disease. This study could be helpful in improving the post-processing quality of medical images, where the false detection occurs due to the presence of noise bursts. The research work is concluded by following suggestions: For future directions, other variants of noises and distributions could be used for image synthesis. The de-noising technique could further be optimized for other dimensions of noisy images. The impact of non-homogeneous noise is not yet explored for image processing. In the future fuzzy rule based thresholding presented in this research will further improve for ridgelets and curvelets. In the future one can possibly investigate how to separate noise burst from edges of malignant area without compromising the pattern.

Acknowledgments

We wish to thank Daniel from Denver, Colorado, USA for facilitating MR images and to the Graduate School of Engineering Sciences and Information Technology, Hamdard University for their logistic support and services.

REFERENCES

1. Mallat, S.G.1989, "A theory for multi-resolution signal decomposition: the Wavelet representation," IEEE Analysis and Mach. Intel., Volume:11 Issue:7,Page(s):674-693.
2. Mallat, S. G. 1998, "A Wavelet Tour of Signal Processing," Academic Press.
3. Ingrid Daubechies.1988, "Orthonormal bases of compactly supported Wavelets," Comm. Pure & Applied Mathematics Page(s):909-996, 1988.
4. Rafeal Gonzalez and R. Wood. 2002, Digital Image Processing, Pearson Education, Inc., 2nd edition.
5. Gilbert Strang and Truong Nguyen, 1996. Wavelets and Filter Banks, by, Wellesley- Cambridge Press.
6. Haar Alfred, 1910. Zur Theorie der orthogonale Frunktionen-Systeme.Math. Annalen Page(s):331- 371.
7. Daubechies Ingrid, 1992. *Ten Lectures on Wavelets*. Philadelphia: Society for Ind. an Applied Mathematics.
8. Cohen, Daubechies I, and J.C. Feauveau.1992, Bi-orthogonal bases of compactly supported Wavelets, Comm. Pure &Applied. Mathematics 45, Page(s):485-560.
9. R.Nowak.1999, "Wavelet-based rician noise removal for magnetic resonance imaging" IEEE Trans.Imag.Proc.,8: Page(s):1408-1419.
10. Héctor Cruz-Enríquez and Juan V. Lorenzo- Ginori. 2009, Combined Wavelet and Nonlinear for MRI Phase Images," ICIAR Page(s):83- 92
11. Edelstein WA, Glover GH, Hardy CJ, Redington RW., 1986 "The intrinsic signal-to-noise ratio in NMR imaging," Magnetic. Resonance. Medical, Volume:3, Page(s):.604-618.
12. Pizurica, et.al, 2006. "A Review of Wavelet de- noising in MRI & Ultrasound brain imaging," Current Medical Imaging Review, 2.2 Page(s): 247-260.
13. R.Archibald and A.Gelb, 2002. "Reducing the effects of noise in MRI reconstruction", Page(s): 497-500.
14. Rashid Hussain and Abdul Rehman Memon , 2011. "Towards an Efficient Segmentation of Malignant Areas in Noisy Brain MR (Magnetic Resonant) Images" Int'l Journal of Acad. Research. Vol. 3 Issue:1 Page(s): 365-375.
15. Rashid Hussain, Sheeraz Arif, M. Ahmed Sikander, and Abdul Rehman Memon , 2011. "Fuzzy clustering based malignant areas detection in noisy breast Magnetic Resonant (MR) images" Int'l Journal of Acad. Research. Vol. 3 Issue:2. Page(s): 64-70.
16. D.L.Donoho, I. M. Johnstone, 1995. "Adapting to Unknown Smoothness via Wavelet Shrinkage," Journal of the American Statistical Association 90(432), Page(s): 1200-1224.